Tunnelling of frequency-modulated wavepackets in photonic crystals with amplification

2016 J. Opt. 18 015102

(http://iopscience.iop.org/2040-8986/18/1/015102)

IOP Publishing Journal of Optics
J. Opt. 18 (2016) 015102 (9pp) doi:10.1088/2040-8978/18/1/015102

Tunnelling of frequency-modulated wavepackets in photonic crystals with amplification

Yu S Dadoenkova[1,2,3], N N Dadoenkova[1,2], D A Korobko[1], I O Zolotovskii[1], D I Sementsov[1] and I L Lyubchanskii[2]

[1] Ulyanovsk State University, 432017, Ulyanovsk, Russian Federation
[2] Donetsk Physical and Technical Institute of the National Academy of Sciences of Ukraine, 83114 Donetsk, Ukraine
[3] Institute of Electronic and Informational Systems, Novgorod State University, 173003 Veliky Novgorod, Russian Federation

E-mail: dadoenkova@yahoo.com

Received 28 June 2015, revised 24 September 2015
Accepted for publication 8 October 2015
Published 24 November 2015

CrossMark

Abstract
The tunnelling of a long-time (about 100 μs) frequency-modulated electromagnetic pulse through a one-dimensional active dielectric photonic crystal and the influence of the frequency modulation of the wavepacket on its time delay and peak velocity is theoretically investigated. The possibility of tuning the characteristics of the transmitted pulse using frequency modulation is demonstrated.

Keywords: photonic crystal, wavepacket, time delay, Hartman effect

(Some figures may appear in colour only in the online journal)

1. Introduction

The tunnelling, or propagation of a quantum particle through a potential barrier with a height larger than the particle's energy, is one of the fundamental quantum effects [1–3]. For calculation of the tunnelling time, the problem is to find out the velocity of a particle in the region where its pulse is imaginary [4, 5]. The calculation of the tunnelling time of a particle according to the stationary phase method leads to the well-known Hartman effect, when the tunnelling time does not exceed some finite value, which for a quite large barrier thickness can result in a superluminar tunnelling velocity of the particles or wavepackets [5–7]. Recently, attention has been paid to investigation of optical soliton propagation [8], and soliton pulse compression, as well as to the development of slow- and fast-light methods for various applications. For many practical reasons, a pulse of light should be delayed by one to several times the pulse duration in a controllable way to find potential application in the fabrication of tunable optical delay lines based on coupled resonator optical waveguides and photonic crystal waveguides, including optical communication systems, random-access memory, network buffering, data synchronization, and pattern correlation [9]. It has been shown that it is possible to delay a pulse by very many pulse lengths [10].

For quite a long time, the interpretation of the Hartman effect has been the subject of intense discussion. As a part of these discussions, a classical optical problem concerning the propagation of electromagnetic waves through macroscopic photonic barriers [7, 11–24] was studied. As an example of such barriers, one-dimensional (1D) photonic crystals (PCs) can be considered, i.e. stratified periodic structures based on materials with different refractive indices. Over the last few decades, such structures have been the focus of intense theoretical and experimental investigations. The periodical modulation of the refractive indices ensures the existence of photonic band gaps (PBGs) in the spectra of the PCs, where the transmittivity is vanishingly small, and the incident radiation is almost totally reflected [25–28]. The propagation of wavepackets within the PBG is similar to the tunnelling process due to similarities in the stationary Schrödinger equation and Helmholtz equation, which describe the spreading of electromagnetic waves in a 1D PC. A comparative study of the propagation of light in the PBGs of a PC with tunnelling through a classically impenetrable barrier is reported in [29]. It should be mentioned that tunnelling effects are common phenomena in wave propagation through periodic structures, for example, acoustic waves in phononic crystals [30].

Analytical and numerical calculations of the wavepacket time delay in 1D PCs have been carried out by many authors [23, 24, 31–35]. A series of experiments on wavepacket propagation in 1D PCs [12–14] confirmed the paradoxical theoretical prediction about the convergence of the wavepacket's time delay to a finite value, which in the limit is independent of the barrier thickness. The interpretation of superluminar tunnelling of the wavepacket as a reshaping of its time envelope (including asymmetric extension or compression of the wavefront, bifurcation and a shift of the wavepacket maximum along the time axis) [15–17] or as a spreading of its different spectral components [18, 19] are under serious criticism [23, 24, 31, 32]. One of the most reasonable interpretations for this effect is that the tunnelling time is not the propagation time, but it is the time for leaking of the energy stored in the barrier [24]. Under this condition, the evanescent modes inside the barrier do not propagate and can be considered as virtual photons not existing beyond its limits [23, 33]. In paper [36], it was shown that the superluminal tunnelling process of a two-dimensional electromagnetic pulse through a 1D PC is the propagation of the net forward-going Pointing vector in a 1D PC.

Although the group velocity of the wavepacket spreading inside a PC can be larger than the speed of light c and can even be negative [21], the velocity of energy propagation never exceeds the vacuum light speed. The appearance of a superluminal advance or subluminal delay of the pulse peak inside a PC or at the exit end is due to wave interference from Bragg reflection [21]. Furthermore, it was shown that pulse coherence can also affect the pulse peak velocity change from superluminal to subluminal in 1D PCs [22]. In addition, an approximate energy, momentum, and form invariance of an ultrashort (about 2 ps) pulse transmitted through a 1D PC at the PBG-edge transmission resonance, and it was demonstrated that a strong transient localization of the optical energy inside the PC provides a large and sensitively adjustable group delay [24]. Recently, the Hartman effect has been theoretically studied in 1D PCs with a defect layer doped by three-level ladder-type atoms [37, 38], where the switching from the positive to negative effect is possible by adjusting the controlling parameter. A similar investigation for case of doping the defect layer with three-level lambda-type atoms was performed in [39].

However, one can point out some incompleteness of these investigations, as their main goals were to solve the paradoxical dependence of the relaxation time, while some application aspects were not considered. Also, the time delay τ_{d} of the transmitted pulse was estimated in terms of the complex transmission coefficient $T(\omega)$ as $\tau = \sqrt{(\partial\phi/\partial\omega)^2\big|_{\omega=\omega_0} + (\partial \ln|T|/\partial\omega)^2\big|_{\omega=\omega_0}}$ with ω_0 being the carrying frequency of the pulse, and the possibility of tuning the time delay of the wavepacket and its peak velocity using the initial frequency modulation (FM) of the input pulse, as well as the influence of the amplification in the PC on the transmitted pulse parameters were not investigated.

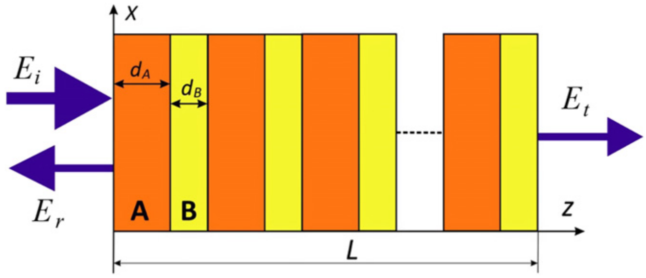

Figure 1. Schematic of the PC with the structure $(AB)^N$. Here E_{i}, E_{r}, and E_{t} denote electric fields of the incident, reflected and transmitted waves, respectively.

In this paper, we investigate the tunnelling of a long-time (about 100 μs) frequency-modulated Gaussian electromagnetic pulse through a 1D active PC. In contrast to the aforementioned publications devoted to different aspects of tunnelling effects in PCs [23, 24, 29, 31–35], our goals are as follows: i) to study the influence of frequency modulation of the incident signal on its time delay; ii) to investigate the role of amplification (which is appropriate for one of the PC layers) in the Hartman effect; iii) to analyze the conditions of sub- and superluminal pulse peak propagation. The paper is organized as follows. In section 2, we describe the propagation of the electromagnetic waves in the 1D PC using a coupled-mode approach and provide a general description of the frequency-modulated wavepacket tunnelling in a 1D PC. In section 3, we show the results of numerical calculations of the time delay of the pulse without FM in an active PC. In section 4, we investigate the influence of the FM on the properties of the pulse transmitted through an active PC. In the conclusion (section 5), we summarize the obtained results.

2. General analysis

2.1. Propagation of electromagnetic waves in a one-dimensional PC

We focus on a finite-size two-component dielectric PC of regular structure $(AB)^N$ with a period $D = d_{\mathrm{A}} + d_{\mathrm{B}}$, where d_{A} and d_{B} are the thicknesses of the layers A and B, respectively. We consider the normal incidence of the electromagnetic waves on the left hand surface of the PC schematically presented in figure 1. The layers of the PC are located parallel to the (xy) plane and are supposed to be infinite in the x- and y- directions, and the z-axis is normal to the interfaces. The total thickness of the PC is $L = DN$. The refractive indices of the PC's constituents are $n_{\mathrm{A}} = n_0 - \tilde{n}$ and $n_{\mathrm{B}} = n_0 + \tilde{n}$, where n_0 is an average refractive index, and $\tilde{n}$ is its deviation.

The periodic variation of the refractive index in the PC can be written as

$$n(z) = n_A + (n_B - n_A) \sum_{m=1}^{N} \Big[\theta\big(md_A - z\big) - \theta\big(md_A + md_B - z\big) \Big]. \quad (1)$$

Here, $\theta(z)$ is the Heaviside step function. Assuming a small difference between the refractive indices of the layers, i.e. $\tilde{n} \ll n_0$, we use the coupled-mode approach [41] to calculate the transmission coefficient. The electric field inside the PC can be presented as a superposition of waves running in opposite directions: $E(z) = E^{+}(z)e^{i\beta z} + E^{-}(z)e^{-i\beta z}$. The periodic variation of the refractive index results in the reflection of the incident wave of magnitude $E^{+}(z)$, running along the z-direction, into the wave $E^{-}(z)$, which propagates in the opposite direction. In turn, this wave reflects into the wave running along the z-axis, etc. The presence of the amplification in the system is taken into account via its average increment α. In this case, the dynamics of the electromagnetic waves can be described by the set of differential equations for their magnitudes:

$$\frac{\partial E^{+}}{\partial z} - \alpha E^{+} = i\sigma E^{+} e^{2i\delta z}, \qquad \frac{\partial E^{-}}{\partial z} + \alpha E^{-} = -i\sigma E^{-} e^{-2i\delta z}, \quad (2)$$

where $\sigma \approx \frac{(n_A + n_B)\omega}{\pi c} \sin\left(\frac{\pi d_A}{D}\right)$ is the coupling constant between the waves propagating parallel and antiparallel to the z-axis, and the parameter $\delta \approx (n_A + n_B)\omega/(2c) - \pi/D$ describes phase synchronism detuning. The boundary conditions for equations (2) can be presented as $E^{+}(0) = E_0$, $E^{-}(L) = 0$. Thus, the transmission coefficient is the ratio of the transmitted and incident wave magnitudes, and it can be written as

$$T = |T| e^{\left(-i\phi_T'\right)} = \frac{s\, e^{\left(-i\beta_0 L\right)}}{s\, ch(sL) - [\alpha - i\delta]\, sh(sL)}, \quad (3)$$

where $s = \sqrt{\sigma^2 + (\alpha - i\delta)^2}$, and $\beta_0 = \omega_B/(2c)$ is the wavevector; the angular frequency ω_B satisfies Bragg's condition for the structure under consideration, and ϕ_T' is the phase of the complex transmission coefficient.

2.2. Tunnelling of the frequency modulated pulse through the photonic crystals

Let us consider a pulse with the time envelope $E(t)$, propagating with the carrier angular frequency ω_0. The time envelope $E_T(t)$ of the transmitted pulse can be calculated using the inverse Fourier transform of the convolution of the initial pulse Fourier transform $\tilde{E}_{in}(\Omega)$ with the complex transmission coefficient $T(\omega)$ as:

$$E_T(t) = \frac{1}{2\pi} \int_{-\infty}^{\infty} \tilde{E}_{in}(\Omega) T\big(\omega_0 + \Omega\big) e^{i\Omega t}, \ \Omega = \omega - \omega_0, \qquad \tilde{E}_{in}(\Omega) = \int_{-\infty}^{\infty} E(t) e^{-i\Omega t} dt. \quad (4)$$

The complex transmission coefficient $T(\omega)$ can be written in the form

$$T(\omega) = e^{\left(-i\phi_T(\omega)\right)} = e^{\left[-i\left(\phi_T'(\omega) - i\phi_T''(\omega)\right)\right]}, \qquad \phi_T''(\omega) = -\ln|T(\omega)|. \quad (5)$$

The approximate expressions for $E_T(t)$ and the pulse time delay for propagation in the PC can be obtained via a Taylor expansion of $T(\omega)$ in the vicinity of the frequency ω_0:

$$\phi_T(\omega) = \phi_T(\omega_0) + \Omega \left. \frac{\partial\left(\phi_T' - i\phi_T''\right)}{\partial\omega} \right|_{\omega=\omega_0} + \frac{\Omega^2}{2} \left. \frac{\partial^2\left(\phi_T' - i\phi_T''\right)}{\partial\omega^2} \right|_{\omega=\omega_0} + \dots \quad (6)$$

Let us assume that the initial Gaussian pulse has the linear chirp $C = a\tau_0^2$ with a constant speed of the FM $a(t) = \text{const}$:

$$E(t) = E_0 \exp\left[-\frac{(1 + iC)t^2}{2\tau_0^2}\right], \quad (7)$$

where τ_0 is the pulse duration. In this case, neglecting the terms of the Taylor series higher than the second order in equation (7), the time envelope of the transmitted pulse has the Gaussian form [42, 43]:

$$\begin{aligned} E_T(t) &= \rho(t) e^{i\Phi(t)}, \\ \rho(t) &= E_0 |T(\omega_0)| \exp\left[K_i^2\left(1 + S^2\right)\tau_p^{-2}\right]\left(\frac{\tau_0}{\tau_p}\right)^{1/2} \times \exp\left[-\frac{\tau_s^2}{\tau_p^2}\right], \\ 2\Phi(t) &= \left[S\tau_s^2 + 2\tau_s K_i\left(1 + S^2\right) + K_i^2 S(1 + S)\right]\tau_p^{-2} - \arctan(S + C) - 2\phi_T'(\omega_0), \end{aligned} \quad (8)$$

$$\begin{aligned} S &= \frac{\left(1 + C^2\right)D_r - C\tau_0^2}{\left(1 + C^2\right)D_i + \tau_0^2}, \\ \chi_1 &= \left(CD_r - D_i\right)\tau_0^{-2}, \ \chi_2 = \left(CD_i - D_r\right)\tau_0^{-2}, \\ \tau_p &= \tau_0^2 \left(\frac{\left(1 - \chi_1\right)^2 + \chi_2^2}{\tau_0^2 + D_i\left(1 + C^2\right)}\right)^{1/2}, \end{aligned} \quad (9)$$

where τ_p is the transmitted pulse duration, $K_i = \frac{\partial\phi_T'}{\partial\omega}$, $K_r = \frac{\partial\phi_T''}{\partial\omega}$, $D_i = \frac{\partial^2\phi_T'}{\partial\omega^2}$, and $D_r = \frac{\partial^2\phi_T''}{\partial\omega^2}$.

A shift of the time envelope's maximum is defined as

$$\tau_s = t - K_i(\omega_0) - SK_r(\omega_0) = t - \left.\frac{\partial \phi'_T}{\partial \omega}\right|_{\omega=\omega_0} - S\left.\frac{\partial\, ln|T|}{\partial \omega}\right|_{\omega=\omega_0}. \quad (10)$$

The position of the carrier frequency in the PBG spectrum of the PC basically defines a shift of the pulse maximum. The time τ_s is analogous to the time in a co-moving frame of reference in a dispersive medium. It should be noted that the second derivatives D_i and D_r are about 10–11 orders less than the first derivatives K_i and K_r. Thus, neglecting the second derivatives in equation (9), one can obtain the parameter $S \approx -C$, and the pulse duration is conserved while transmission through the PC: $\tau_p = \tau_0$.

In [23, 33–35, 40] the time delay of the pulse transmitted through the PC was calculated neglecting the third term $(\partial \ln|T|/\partial\omega)|_{\omega=\omega_0}$ in equation (10), which tends to zero for pulses without chirp and for frequencies far from the PBG edge. In this case, the time delay can be written as:

$$\tau_d = \left.\frac{\partial \phi'_T}{\partial \omega}\right|_{\omega=\omega_0}. \quad (11)$$

Taking into account equation (3), the time delay τ_d inside the PBG ($\delta < \sigma$) for the passive PC ($\alpha = 0$) can be written as [33]:

$$\tau_d = \frac{n_0 L}{c}\left[\frac{(\sigma/s)^2 \tanh(sL)/sL - (\delta/s)^2\, \mathrm{sech}^2(sL)}{1 + (\delta/s)^2 \tanh^2(sL)}\right]. \quad (12)$$

In the limiting case of an infinite barrier $L \to \infty$, the time delay converges to the finite quantity $\tau_d = n_0/(sc)$, and in the PBG center (for $\delta = 0, \alpha = 0$) the time delay is $\tau_d = n_0/(\sigma c) = \Omega_c^{-1}$, where Ω_c is the PBG width. The infinite tunnelling speed paradox can be solved so that the time delay should not be considered as the time of the pulse transmission through the barrier. The spatial size of the pulse is larger than the barrier width L, and the pulse propagates quasi-statically. As a result, the field distribution inside the barrier is stationary. In this sense, the PC has an analogy to a capacitor, and the time delay is the ratio between the average stored energy and the input power [44]. The radiation energy inside the PBG is concentrated near the barrier surface, and the energy density decays rapidly with the barrier length. Thus, the energy stored in the PC for relatively large L tends to a finite value, i.e. the PC becomes saturated. It is precisely this fact that explains the time delay saturation.

3. Time delay of a pulse without frequency modulation in active photonic crystals

First, we focus our investigation on the influence of amplification on the spectrum of the PC and on the time delay of the pulse without a chirp, which is tunnelling through such a system. Next, we will compare these results with those obtained for pulses with FM.

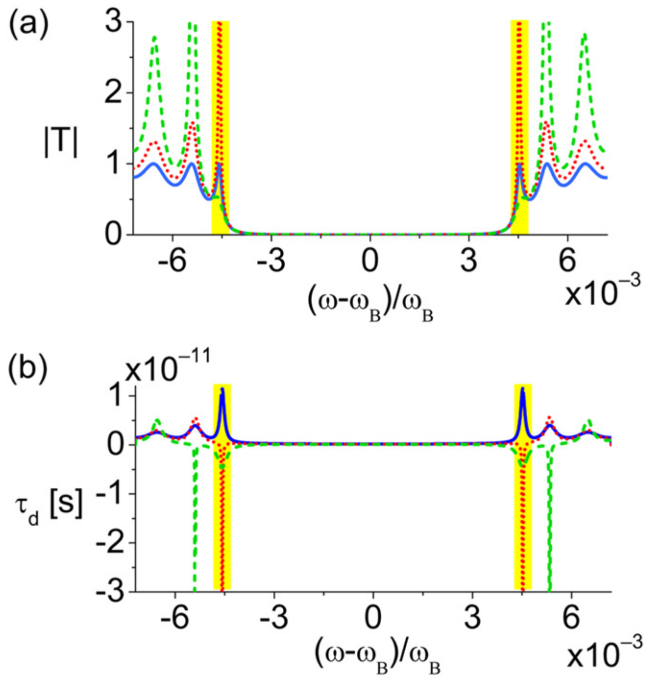

Figure 2. Spectra of the absolute values of the transmission coefficients $|T(\omega)|$ (a) and the time delay τ_d of the transmitted pulse (b) for the passive PC ($\alpha = 0$) (solid lines) and for the active PC with the amplification coefficients $\alpha L = 0.15$ and $\alpha L = 0.45$ (dotted and dashed curves, respectively).

The time delay τ_d in the middle of the PBG does not change in essence while taking into account the amplification in the active PCs. The Bragg reflection does not allow penetration of the radiation of the angular frequencies $\omega \approx \omega_B$ in the depths of the structure, and the energy capacity of the PC at these frequencies practically does not change. On the other hand, at the PBG edges, one can observe effects related to changing τ_d. For ω_B near these frequencies, the derivative $(\partial \ln|T|/\partial\omega)|_{\omega=\omega_0}$ cannot be neglected, and in this case, for the calculation of τ_d, one should use equation (10). However, for pulses without FM, the parameter $S \ll 1$ [see the equation (9)], and the time delay of the transmitting pulse maximum can be estimated by equation (11).

Figure 2 shows the transmission spectra $|T(\omega)|$ and the time delay τ_d calculated according to equation (11) for the passive and active PCs illustrated in figure 1 with the material parameters $n_0 = 3$ and $\tilde{n} = 0.02$. These values correspond to typically used semiconductor structures based on $Al_{0.7}Ga_{0.3}As$ at the angular frequency $\omega_B = 1.2566$ rad · PHz, corresponding to a wavelength of about 1.5 μm [45]. The thicknesses of the layers A and B are $d_A = 124.2$ nm and $d_B = 125.8$ nm, and the number of periods of the PC is $N = 600$. The solid lines show the transmission characteristics of the passive PC ($\alpha = 0$), the dotted and dashed curves correspond to ones for the PC with the amplification coefficients $\alpha L = 0.15$ and $\alpha L = 0.45$, respectively. For these parameters, the PBG width is approximately $\Omega_c \approx 0.009\omega_B$, or 11.31 rad · THz. As one can see from equation (3), when the coupling constant σ of the waves propagating parallel and antiparallel to the z-axis becomes equal to the phase synchronism detuning parameter δ, the spectrum of the complex transmission coefficient $T(\omega)$ of the passive PC exhibits a singular point where the denominator of equations (3) turns to zero; thus $|T| \to 0$, so the energy output does not need the presence of the input radiation, i.e. generation takes place. It should be noted that every singular point corresponds to one of the modes of the distributed feedback laser [41]. At the generation point, the time delay increases to infinity, because the PC radiates at zero input energy. The increase of the amplification leads to a shift of the singular point of $T(\omega)$ towards higher frequencies at the high-frequency PBG edge, corresponding to $\delta > \sigma$, while at the low-frequency PBG edge the singular point shifts to lower frequencies (see the dashed lines in figure 2).

From equation (12), it follows that for the passive PC in the frequency region where $\delta \to \sigma$, the time delay of the transmitted pulse increases up to the value corresponding to the transmission time of the electromagnetic waves propagating through the PC with the velocity of light in the medium, $t_d = n_0 L/c$. In the active PC, τ_d increases in the spectral bands which correspond to $\delta \approx \sigma$. This fact can be explained by a significant penetration of the radiation of the frequency at which $\delta = \sigma$ into the structure, as well as by multiple reflections in this band and by the increasing of the energy capacity of the PC.

It should be noted that in the frequency region before the singular point, the phase ϕ'_T changes rapidly, and its derivative $\partial\phi'_T/\partial\omega$ can change its sign, which means the possibility of negative values of τ_d.

According to equation (10), the time delay depends on dispersion of the transmission coefficient's phase $(\partial\phi'/\partial\omega)|_{\omega=\omega_0}$. Taking into account the term $-S(\partial \ln|T|/\partial\omega)|_{\omega=\omega_0}$ in equation (10), one can see that not only the parameters of the PC define the value of τ_d, but also the initial properties of the pulse do, particularly, its frequency modulation, i.e., the chirp.

4. Time delay of a frequency modulated pulse transmitted through photonic crystals

In this section, we investigate the influence of the input pulse's chirp on the transmitted pulse properties. We solve equation (2) for a Gaussian input pulse defined by equation (4) for the pulse duration $\tau_0 = 10^{-4}$ s with the linear FM $C \sim 10^8$, and compare the results with those obtained for the pulse without FM, but with the same spectrum width. The duration of such a pulse without FM is can be estimated using $\tau'_0 = \tau_0\sqrt{1 + C^2} \approx \tau_0/C = 10^{-12}$ s.

Figures 3(a) and (b) show the normalized spectral densities of the pulses for the FM speed $a = 10^{15}$ s^{-2} and $a = 10^{16}$ s^{-2}, respectively. The solid lines correspond to spectral densities $|\tilde{E}_{in}(\Omega)|/|\tilde{E}_{in}^{max}(\Omega)|$ of the input pulses, and the dashed, dash-dotted and dotted lines correspond to spectral densities $|\tilde{E}_T(\Omega)|/|\tilde{E}_{in}^{max}(\Omega)|$ of the transmitted pulses for the PC with the amplification parameters $\alpha = 0$, $\alpha L = 0.15$, and $\alpha L = 0.45$. The carrier frequency of the input pulse $\omega_0 = 1.2623$ rad · PHz is close to the PBG edge, and the duration of the input pulse is $\tau_0 = 10^{-4}$ s. The yellow areas show the PBG.

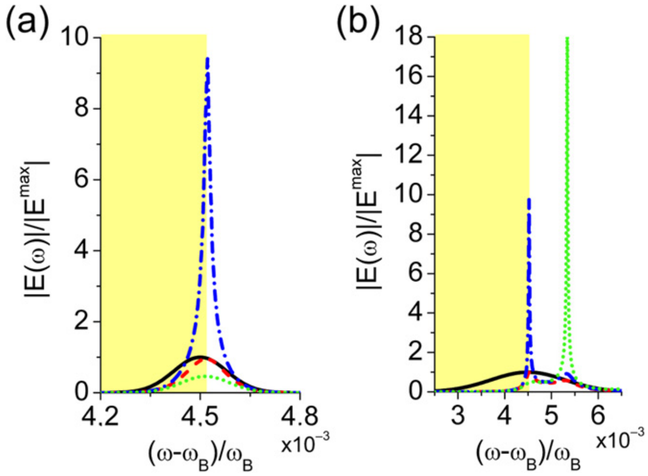

Figure 3. The normalized spectral densities $|\tilde{E}_{in}(\Omega)|/|\tilde{E}_{in}^{max}(\Omega)|$ and $|\tilde{E}_T(\Omega)|/|\tilde{E}_{in}^{max}(\Omega)|$ of the input (solid lines) and transmitted pulses for the PC with the amplification coefficients $\alpha = 0, \alpha L = 0.15$ and $\alpha L = 0.45$ (dashed, dash-dotted and dotted lines, respectively), for the modulation speed $a = 10^{15}$ s^{-2} (a) and $a = 10^{16}$ s^{-2} (b). The carrier frequency of the input pulse is $\omega_0 = 1.2623$ rad · PHz , and the input pulse duration is $\tau_0 = 10^{-4}$ s. The yellow areas show the PBG.

For the input pulse with FM speed $a = 10^{15}$ s^{-2}, the increase of the amplification coefficient leads to a decrease of the $\tilde{E}_T(\Omega)$ peak at the PBG edge (see figure 3(a)), as the singular point discussed above shifts towards higher frequencies (see figure 2(a)) and the high-frequency component of the pulse is not enhanced much. For the pulse with a larger chirp, $a = 10^{16}$ s^{-2}, the high-frequency component of the pulse is enhanced at the transmission, as one can see from comparison of the dashed, dash-dotted and dotted lines in figure 3(b). This fact results in the appearance of a second peak at a frequency higher than the frequency of the PBG edge. Comparing the dotted curves in figures 3(a) and (b) one can see that the pulse with relatively small chirp transmits without any strong reshaping.

We restrict further consideration to the case when the input Gaussian pulse is narrow enough to exclude strong reshaping of its leading front at transmission, as discussed above. It should be noted that equation (10) for the time delay is inapplicable for strong transmitted pulse reshaping because the time envelope shape is no longer a Gaussian one, as it was assumed while deriving the analytical expression in equation (10).

It should be noted that in accordance with the fact that the transmitted pulse spectrum is defined by both the input pulse spectrum and the transmission spectrum $|\tilde{E}_{out}(\Omega)|/|\tilde{E}_{in}(\Omega)T(\Omega)|$, the coincidence of the spectral densities of the input pulses $|\tilde{E}_{in}(\Omega)|$ with and without chirp results in the coincidence of the spectral densities of the corresponding transmitted pulses. Thus, the pulses with

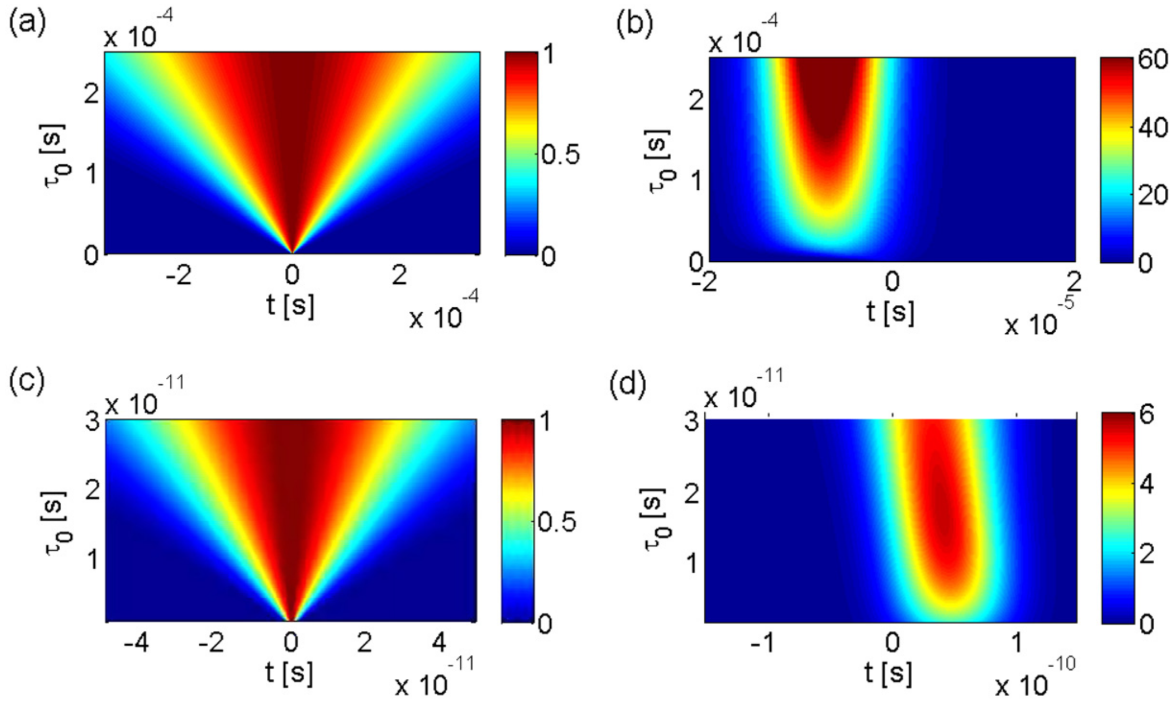

Figure 4. Color plot of the time envelopes $E(t)/E_0$ evolution with the incident pulse duration τ_0: the input pulse with the FM speed $a = 5 \cdot 10^{15}\ \mathrm{s}^{-2}$ (a) and the short-time input pulse without a chirp (c) (here the input pulse duration range corresponds to the one for the pulse with a chirp with the same spectral width); the transmitted pulse with chirp (b) and without chirp (d). The carrier frequency of the input pulse is at the PBG edge $\omega_0 = 1.2623$ rad · PHz. The color depicts the values of $E(t)/E_0$.

different chirps but with equal spectrum widths are indistinguishable. However, the difference in the phase of $\tilde{E}_{\mathrm{in}}(\Omega)$ leads to significant differences in the forms of the time envelopes $E_{\mathrm{T}}(t)$ of the transmitted pulses.

This situation is illustrated in figure 4, where we present the evolution of the dimensionless time envelopes with the time and input pulse duration τ_0 for an equal spectrum of incident pulses with and without chirp (figures 4(a)–(d)). The color depicts the values of the normalized time envelope of the input $E_{\mathrm{in}}(t)/E_0$ (figures 4(a) and (c)) and transmitted pulses $E_{\mathrm{out}}(t)/E_0$ (figures 4(b) and (d)) for the carrier frequency $\omega_0 = 1.2623$ rad PHz at the high-frequency PBG edge. The FM speed is $a = 5 \cdot 10^{15}\ \mathrm{s}^{-2}$, and the amplification coefficient is $\alpha L = 0.15$.

Both pulses (with and without chirp) initially have their spectral components enhanced in the active PC. In the case of the pulse with a chirp (figure 4(b)) these components belong to the leading edge of a long-time input pulse (figure 4(a)). The transmitted pulse loses its low-frequency components filtered by the structure. Consequently, one can see that the transmitted pulse maximum is located before the maximum of the input pulse, i.e. the negative time delay of the transmitted pulse takes place (compare figures 4(a) and (b)). The time envelope reshaping is caused not only by the amplification in the PC but also by the filtration of the spectral components distributed over a period of the pulse. For the reversed linear FM ($C < 0$), the time delay is positive, caused by the cut-off of the leading edge of the pulse and the enhancement of the trailing edge of the pulse. The time delay depends on the chirp, thus equation (11) cannot be used any more for the calculation of τ_{d}. In the first approximation, one can use equation (10). It should be mentioned that the transmitted pulse duration is less than the duration of the input pulse. Only conventionally, this fact can be treated as 'compression', as the transmitted pulse is not a complete transformation of the input one. The origin of the 'compression' is connected to the fact that the transmitted frequency band is localized in a narrow time interval on the leading edge of the pulse.

Considering the transmission of a more short-time pulse but without a chirp (see figures 4(c) and (d)), it should be noted that the time delay is only defined by the dispersion of the complex transmission coefficient $T(\omega)$. The transmitted spectral components are uniformly distributed by the incident pulse duration. In the course of multiple reflections inside the PC, the transmitted pulse is formed on the basis of these components. Due to the dispersion of $T(\omega)$, the transmitted pulse suffers dispersion spreading and becomes frequency-modulated. A significant spectrum narrowing of the transmitted pulse in comparison to the input pulse, along with dispersion spreading, causes the increase of the transmitted pulse duration (compare figures 4(c) and (d)). As it has been mentioned above, the time delay of the transmitted pulse's maximum can be estimated using equation (11). Due to amplification of the PC, the peak power of the transmitted pulse is larger than the peak power of the input pulse (see figures 4(a)–(d)).

Thus, the FM of the pulse makes it possible to reverse the time delay of the transmitted pulse and to decrease its duration, in contrast to the pulse without a chirp.

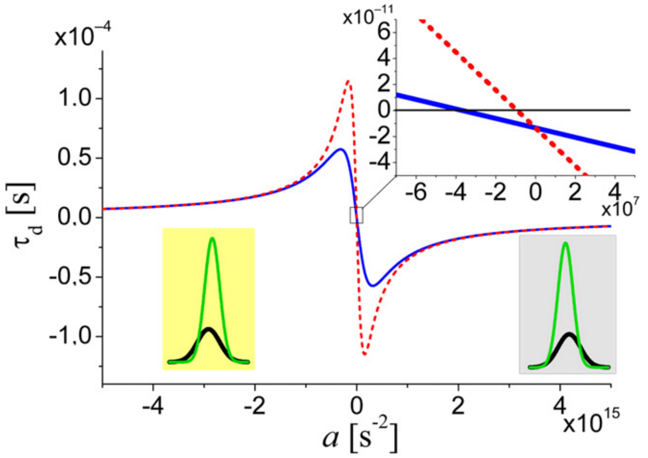

Figure 5. The time delay τ_d of the transmitted pulse as a function of the FM speed a for the input pulse durations $\tau_0 = 10^{-4}$ s (the solid lines) and $\tau_0 = 2 \cdot 10^{-4}$ s (the dashed lines) for $\omega_0 = 1.2623$ rad · PHz. The insets demonstrate the typical time envelopes of the input and transmitted pulses (the bold and narrow lines, respectively) in each region shown with yellow and gray areas.

Figure 5 presents the time delay τ_d of the Gaussian pulse as function of the FM speed a for two values of the input pulse duration $\tau_0 = 10^{-4}$ s and $\tau_0 = 2 \cdot 10^{-4}$ s (the solid and dashed lines, respectively). The amplification coefficient of the PC is $\alpha L = 0.15$, and the carrier frequency of the pulse at the PBG edge is $\omega_0 = 1.2623$ rad · PHz. One can single out two regions of a where the characteristics of the transmitted pulse are similar. In accordance with the discussion presented above, the pulse with a positive chirp (i.e., $a > 0$) suffers a negative time delay. However, $\tau_d < 0$ can occur for negative FM speed as well until the third term in equation (10), $S(\partial \ln|T|/\partial\omega)|_{\omega=\omega_0}$, starts to have a significant impact on τ_d. The component of the shift, which is proportional to $\partial\phi_T'/\partial\omega$, does not depend on the chirp and its value is about 10^{-11} s (see figure 2(b)). This term dominates in the case of small chirp. It should be noted that for the pulse with $\tau_0 = 10^{-4}$ s ($\tau_0 = 2 \cdot 10^{-4}$ s), the time delay is positive for the negative FM speed until $a = -3.7 \cdot 10^7$ s^{-2} ($a = -0.9 \cdot 10^7$ s^{-2}), as one can see from the upper inset in figure 5. In the absence of the FM ($a = 0$) the time delay is negative. The lower insets in figure 5 show the typical relations between the peak power of the input (the bold black lines) and transmitted (the narrow lines) pulses (the proportions are not kept) for each region of the τ_d with similar behavior: yellow and grey areas correspond to $\tau_d > 0$ and $\tau_d < 0$, respectively.

The dependence of the time delay on the FM speed is not monotonic. Firstly, the absolute value of τ_d increases with the increase of $|a|$. In this region of the FM speed, the time envelope of the transmitted pulse forms due to the dispersion shift of the tunnelling Gaussian pulse. The further increase of the absolute value of the FM speed ($|a| > 10^{14}$ s^{-2}) leads to a decrease of $|\tau_d|$. Such behavior can be explained as follows: the time coordinate of the transmitting frequency components of the pulse with the increase of the chirp is approaching the input pulse maximum (at $t = 0$). For $|a| > 5 \cdot 10^{15}$ s^{-2} (for the system under consideration) the spectral components, which belong to a narrow part of the input pulse front, are broadening, and the influence of the dispersion shift on τ_d becomes negligible. As a result, the shape of the transmitted pulse deforms and the second peak emerges (see figure 3(b)). Thus, the change of the FM speed allows tuning of the time delay of the transmitted pulse.

The chirp of the pulse can be also changed by variation of the input pulse duration. One can see that the increase of τ_0 leads to an increase of the absolute value of τ_d for $|a| < 0.75 \cdot 10^{15}$ s^{-2}. For large values of the FM speed, the influence of τ_0 on τ_d is negligible. It should be noted that the increase of the input pulse duration decreases the value of a, which corresponds to non-Gaussian deformation of the transmitted pulse.

The defined value of the pulse time delay allows estimation of the velocity of the pulse peak propagation through the PC of thickness L as $V_m = L/t_m$. Time t_m is the time at which the energy density reaches a maximum, and is related to the time delay via $\tau_d = t_m - t_{vac}$, where t_{vac} is the propagation time of the electromagnetic wave through the same distance L in a vacuum. It is well-known that in the vicinity of the PBG edge, the group velocity of the electromagnetic wave drops down [28, 31] to values much less than the speed of light in a vacuum. It should be pointed out that, in general, superluminal wavepackets' appearance is related to pulses with quite a flat leading edge, e.g., to exponential-shaped pulses [46]. Nevertheless, using FM of the Gaussian pulse, it is possible to increase V_m and even to exceed the speed of light in a vacuum. The superluminal peak propagation takes place when $|t_m| < t_{vac}$. Taking into account equations (9) and (10), one can find the region of the FM speed, where $V_m > c$:

$$\frac{\partial\phi'/\partial\omega}{\tau_0^2\,(\partial \ln|T|/\partial\omega)} < a < \frac{2t_{vac} + \partial\phi'/\partial\omega}{\tau_0^2\,(\partial \ln|T|/\partial\omega)}. \tag{13}$$

For the system under consideration, for ω_0 at the high-frequency PBG edge and $\tau_0 = 10^{-4}$ s, the condition equation 13 is satisfied within the interval $-3.6717 \cdot 10^7$ s$^{-2} < a < -3.3967 \cdot 10^7$ s^{-2}, as shown by the yellow areas in figure 6. As one can see from figure 6, the peak velocity can be both positive and negative. The latter happens when the maximum of the transmitted pulse forms before the input pulse peak is formed [46–48]. In the vicinity of $\tau_d = -t_{vac}$ (i.e. when $t_m = 0$) V_m demonstrates rapid growth with the FM speed increase, and the discontinuity and sign change of V_m takes place (see inset in figure 6). It should be noted that the superluminal peak propagation does not contradict the special relativity postulate, as the information about the signal transfers on its leading edge. Outside the aforementioned interval, the peak propagation is subluminal, and further increase of $|a|$ leads to V_m decay, which is in agreement with previous results [28, 31].

5. Conclusions

To conclude, the results of our investigations are as follows. I We have shown that the presence of amplification in a

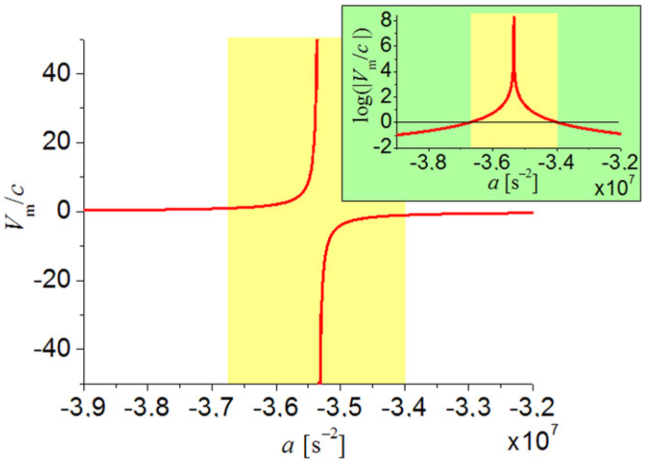

Figure 6. The normalized peak velocity V_m/c as a function of the FM speed. The input pulse duration is $\tau_0 = 10^{-4}$ s and the carrier frequency is $\omega_0 = 1.2623$ rad · PHz. The inset show $|V_m/c|$ in logarithmic scale.

photonic crystal can lead to a negative time delay of the transmitted pulse, even in the absence of frequency modulation, due to reshaping of the time envelope of the input wavepacket. II. Changing the frequency modulation, one can effectively tune the time delay of the transmitted pulses, in particular it is possible to realize both positive and negative time delay. III. In addition, we established values of the frequency modulation speed which correspond to superluminal peak pulse propagation of the tunnelled pulse. Switching of the pulse time delay can be useful for fabrication of optoelectronic emission control devices. The most promising of them are devices which realize controllable pulse delay. Such devices are used in different optoelectronic circuits. We also estimated the values of the frequency modulation speed which correspond to changing of the pulse peak velocity behavior from subluminal to superluminal.

Acknowledgments

This research has received funding from the European Union's Horizon 2020 research and innovation program under the Marie Skłodowska-Curie grant agreement No. 644348, project 'MAGIC' (N N D, Yu S D, and I L L), and COST Action MP1403 'Nanoscale Quantum Optics' (N N D, Yu S D, and I L L) and also is supported by grants from the Ministry of Education and Science of Russian Federation: Project No. RFMEFI57414X0057 (Yu S D, N N D, I O Z, D A K, and D I S). I L L is grateful to Ulyanovsk State University for the hospitality expressed during his stay in Ulyanovsk.

References

[1] Landau L D and Lifshitz E M 1977 *Quantum Mechanics* (*Non-relativistic theory*), *Course of Theoretical Physics* vol 3 3rd ed (Oxford: Butterworth-Heinemann)
[2] Messiah A 1967 *Quantum Mechanics* (Amsterdam: North Holland Publishing Company)
[3] Muga J G and Leavens C R 2000 *Phys. Rep.* **338** 358
[4] MacColl L A 1932 *Phys. Rev.* **40** 621
[5] Shvartsburg A B, Marklund M, Brodin G and Stenflo L 2008 *Phys. Rev. E* **78** 016601
[6] Hartman T E 1962 *J. Appl. Phys.* **33** 3427
[7] Steinberg A M, Kwiat P G and Chiao R Y 1993 *Phys. Rev. Lett.* **71** 708
[8] Zolotovskii I O and Sementsov D I 2000 *Opt. and Spectr* **88** 560
[9] Melloni A, Canciamilla A, Ferrari C, Morichetti F, O'Faolain L, Krauss T F, De La Rue R, Samarelli A and Sorel M 2010 *IEEE Photonics J.* **2** 181
[10] Boyd R W, Gauthier D J, Gaeta A L and Willner A E 2005 *Phys. Rev. A* **71** 023801
[11] Olkhovsky V S and Recami E 1992 *Phys. Rep.* **214** 339
[12] Spielmann Ch, Szipöcs R, Stingl A and Krausz F 1994 *Phys. Rev. Lett.* **73** 2308
[13] Longhi S, Marano M, Laporta P and Belmonte M 2001 *Phys. Rev. E* **64** 055602
[14] Hache A and Poirier L 2002 *Appl. Phys. Lett.* **80** 518
[15] Chiao R Y and Steinberg A M 1997 Tunnelling times and superluminality *in Progress in Optics* ed E Wolf vol XXXVII (Amsterdam: Elsevier)
[16] Nasedkina Yu F and Sementsov D I 2006 *Opt. and Spectr* **100** 776
[17] Zolotovskii I O, Minvaliev R N and Sementsov D I 2010 *Opt. and Spectr* **109** 584
[18] Büttiker M 1983 *Phys. Rev. B* **27** 6178
[19] Landauer R and Martin T 1992 *Solid State Comm* **84** 115
[20] D'Aguanno G, Mattiucci N, Scalora M, Bloemer M J and Zheltikov A M 2004 *Phys. Rev. E* **70** 016612
[21] Liu N-H, Sh-Y Zhu, Chen H and Wu X 2002 *Phys. Rev. E* **65** 046607
[22] Wang Li-gang Liu, Nian-hua Lin, Qiang and Shi-yao Zhu 2004 *Phys. Rev. E* **70** 016601
[23] Winful H 2006 *Phys. Rep.* **436** 1
[24] Scalora M *et al* 1996 *Phys. Rev. E* **54** R1078
[25] Joannopoulos J, Meade R and Winn J 1995 *Photonic Crystals* (Princeton, NJ: Princeton University Press)
[26] Sakoda K 2001 *Optical Properties of Photonic Crystals* (Berlin: Springer)
[27] Lyubchanskii I L, Dadoenkova N N, Lyubchanskii M I, Shapovalov E A and Rasing Th 2003 *J. Phys. D: Appl. Phys* **36** R277
[28] Inoue K and Ohtaka K 2010 *Photonic Crystals: Physics, Fabrication and Applications* (Berlin: Springer)
[29] Solli D R, Morehead J J, McCormick C F and Hickmann J M 2008 J. Opt. A *Pure Appl. Opt.* **10** 075204
[30] Peng P, Ch Qiu, Ding Y, Zh He, Yang H and Liu Zh 2011 *Sol. St. Comm.* **151** 400
[31] Doiron S, Haché A and Winful H G 2007 *Phys. Rev. A* **76** 023823
[32] Winful H G 2003 *IEEE J. Sel. Top. Quantum Electron.* **9** 17
[33] Winful H G 2006 *New J. Phys.* **8** 101
[34] Esposito S 2001 *Phys. Rev. E* **64** 026609
[35] Pereyra P and Simanjuntak H P 2007 *Phys. Rev. E* **75** 056604
[36] Wang L-G and Zhu Sh—Y 2006 *Phys. Rev. B* **73** 195119
[37] Sahrai M, Aghaei R, Sattary H and Poursamad J 2015 *J. Opt. Soc. Am.* B **32** 751
[38] Sahrai M, Aas S, Aas M and Mahmoudi M 2011 *Eur. Phys. J.* B **83** 337
[39] Sahrai M and Esfahlani B 2013 *Physica* E **47** 66
[40] Endo R and Saito R 2011 *J. Opt. Soc. Am.* B **28** 2537
[41] Yariv A and Yeh P 1984 *Optical Waves in Crystals* (New York: Wiley)
[42] Zolotovskii I O and Sementsov D I 2004 *Quantum Electron.* **34** 852

[43] Zolotovskii I O and Sementsov D I 2005 *Opt. and Spectr* **99** 81
[44] Winful H 2002 *Opt. Express* **10** 1491
[45] Pikhtin A N and Yas'kov A D 1980 *Sov. Phys. Semicond* **14** 389
[46] Oraevskii A N 1998 *Phys. Usp* **41** 1199
[47] Akulshin A M, Cimmino A and Opat G I 2002 *Quantum Electron.* **32** 567
[48] Akulshin A M, Cimmino A, Sidorov A I, Hannaford P and Opat G I 2003 *Phys. Rev.* A **67** 011801(R)